

# Non-Abelian Self-Correcting Quantum Memory

Po-Shen Hsin<sup>1,2</sup>, Ryohei Kobayashi<sup>3</sup> and Guanyu Zhu<sup>4</sup>

<sup>1</sup> *Mani L. Bhaumik Institute for Theoretical Physics, 475 Portola Plaza, Los Angeles, CA 90095, USA*

<sup>2</sup> *Department of Mathematics, King's College London, Strand, London WC2R 2LS, UK.*

<sup>3</sup> *Department of Physics, Condensed Matter Theory Center, and Joint Quantum Institute, University of Maryland, College Park, Maryland 20742, USA*

<sup>4</sup> *IBM Quantum, T.J. Watson Research Center, Yorktown Heights, NY 10598 USA*

## Abstract

We construct a family of infinitely many new candidate non-Abelian self-correcting topological quantum memories in  $D \geq 5 + 1$  spacetime dimensions without particle excitations using local commuting non-Pauli stabilizer lattice models and field theories of  $\mathbb{Z}_2^3$  higher-form gauge fields with nontrivial topological action. We call such non-Pauli stabilizer models magic stabilizer codes. The family of topological orders have Abelian electric excitations and non-Abelian magnetic excitations that obey Ising-like fusion rules, generalizing the dihedral group  $\mathbb{D}_8$  gauge theory in 2+1d. The simplest example includes a new non-Abelian self-correcting memory in 5+1d with Abelian loop excitations and non-Abelian membrane excitations. We use a Peierls argument to demonstrate the self-correction property and the thermal stability, and devise a probabilistic local cellular-automaton decoder.

Tuesday 21<sup>st</sup> May, 2024

# Contents

<b>1</b>	<b>Introduction</b>	<b>2</b>
1.1	The model . . . . .	4
1.2	Review of quantum memory at finite temperature for loop toric code . . . . .	5
<b>2</b>	<b>Cubic Theory in <math>D</math> dimension as Non-Abelian TQFT</b>	<b>6</b>
2.1	The model . . . . .	6
2.2	Hilbert space of TQFT . . . . .	6
2.3	Operators . . . . .	7
2.4	Lattice model . . . . .	8
2.4.1	Commuting non-Pauli stabilizer lattice model . . . . .	9
2.5	Cubic theories without particles . . . . .	11
2.6	Cubic theory from compactification of generalized color code . . . . .	12
<b>3</b>	<b>Self-Correcting Cubic Theory of Strings and Membranes</b>	<b>15</b>
3.1	TQFT Hilbert space . . . . .	15
3.2	Operators . . . . .	15
3.3	Commuting non-Pauli stabilizer lattice Hamiltonian model . . . . .	16
3.3.1	Operators on the lattice . . . . .	16
3.3.2	Code distance . . . . .	17
3.4	Non-Abelian braiding of magnetic operators . . . . .	17
3.5	Self-correcting quantum memory . . . . .	19
3.5.1	Readout of the memory and decoding the logical information . . . . .	22
3.5.2	Generalization: general cubic theory without particles . . . . .	22
<b>4</b>	<b>Discussion and Outlook</b>	<b>23</b>
<b>A</b>	<b>Obstruction to Non-Abelian Fusion</b>	<b>24</b>
<b>B</b>	<b>Review of Cup Product on Triangulated and Hypercubic Lattices</b>	<b>25</b>

<b>C Logical CZ, S, Hadamard Gates in 4D Loop Toric Code</b>	<b>26</b>
C.1 Hadamard gate . . . . .	26
C.2 CZ and S gates . . . . .	27

# 1 Introduction

In this work we will investigate the self-correcting property and thermal stability of a family of non-Abelian topological quantum field theories (TQFTs) in higher dimensions. In  $D = 3$  spacetime dimension, the TQFT is the non-Abelian  $\mathbb{D}_8$  gauge theory, i.e. dihedral group of order 8. The theory is recently realized in experiment [1]. It is known that  $D = 3$  TQFTs do not provide self-correcting quantum memory at finite temperature [2–5], while loop toric code TQFT in 4+1d that have only loop excitations is known to be thermally stable quantum memory. However, the loop toric code model describes an Abelian topological order, while non-Abelian topological orders are more useful to implement source-effective logical gates. This motivates us to explore higher dimensional non-Abelian topological order.

Higher dimensional topological orders above the physical dimension can be realized using long-range connections and are relevant for practical fault-tolerant quantum computation [6–8], and they are ubiquitous in quantum low-density parity-check (LDPC) codes [9–21]. Non-Abelian topological orders above  $D = 4$  dimension are less understood except for topological orders with particles (see e.g. [22]), where the particles arise from the electric charges due to gauging an ordinary symmetry. However, such theories with particles cannot provide self-correcting quantum memory at finite temperature (e.g. [2–5, 23]). Thus we will in particular study non-Abelian topological orders without particles. This will also help to answer a fundamental question: whether non-Abelian topological order exists at finite temperature.

From the perspective of practical fault-tolerant quantum computation, a fundamental question is about the space-time overhead for the computation, including the overhead for both the quantum and classical operations in the computing process. In a typical case of an actively corrected quantum memory, one measures the error syndrome and then sends the syndrome information to the classical computer to decode it. The classical decoder then decides a recovery operation to correct the errors. These processes need non-local classical communications and the classical decoder requires computation time scaled with the system size. Since classical communication and gates are not infinitely faster than the quantum gates, such classical time overhead will make it impossible for the classical decoder to keep up with the advancing of quantum operations and to correct the errors timely when the

system is large enough [24,5]. Self-correcting memory is hence more desirable since it gets rid of the classical software and the associated time overhead and instead passively protects the quantum hardware from the errors. While such a passive protection might be challenging at the current stage from the engineering perspective, self-correcting memory is also useful even in the context of active error correction since it is always closely associated with an underlying local cellular-automaton decoder [25,5]. Such a decoder is composed of local update rules at each time step and does not require non-local classical communication. It also does not have a decoding time overhead during the computation process except the final readout stage when the classical decoder no longer needs to catch up with the quantum operations. Although existing single-shot error correction schemes permit constant quantum time overhead [26], only self-correcting quantum memory can potentially achieve both constant quantum and classical time overhead. In fact, there exists a scheme for implementing universal logical gate set with constant-depth geometrically non-local circuits acting on a non-Abelian topological code [27–29] where the time overhead is expected to be  $O(d/\log d)$  ( $d$  is the code distance) due to the stretching of the support of error clusters by a constant factor. If such a scheme can be adapted to a non-Abelian self-correcting memory where the stretched error can be shrunk back in constant time, constant time overhead will be achieved for both the quantum and classical operations during the computation stage.

Although the loop toric code in four space dimension is a self-correcting memory, it only support logical Clifford gates similar to the toric code in two space dimension. On the other hand, universal logical gate set has been found using a generalized color code in six spatial dimensions [30], which also serves as a self-correcting memory. In this work, we have discovered a non-Abelian self-correcting memories in five spatial dimensions, which can potentially allow a universal quantum computing scheme with lower space overhead than the 6D color code scheme. Interestingly, we find that our 5D non-Abelian self-correcting memory can also be obtained from a twisted compactification of the 6D color code in Ref. [30] down to five spatial dimensions. We also generalize the 5D non-Abelian self-correcting memory to a family of infinitely many non-Abelian self-correcting memories above five spatial dimensions.

Topological orders without particles are highly constrained: the lowest-dimensional excitations must obey Abelian fusion rule (see e.g. [31, 32]). For instance, if the lowest-dimensional nontrivial excitation is a membrane, then it must be obey Abelian fusion rule. On the other hand, when there exist nontrivial loop excitations, the membrane excitations do not need to obey Abelian fusion, and they can be non-Abelian. Non-Abelian TQFTs without particles can only exist at or above spacetime dimension  $D \geq 5 + 1$ . To see this, we note that non-Abelian fusion of  $k$ -dimensional excitations with  $k \geq 1$  requires  $(k - 1)$ -dimensional excitations in order to produce a consistent fusion rule after shrinking the  $k$ -dimensional excitations on a circle: without nontrivial  $(k - 1)$ -dimensional excitations, shrinking on a circle would produce the inconsistent fusion  $1 \times 1 = 1 + 1 + \dots$  from the non-Abelian fusion of

$k$ -dimensional excitations (see e.g. [31,32] and appendix A). In addition, we require  $(k-1) \geq 1$  to avoid particles. Remote detectability, i.e. an  $n$ -dimensional excitation must have mutual braiding with some  $(D-n-3)$ -dimensional excitations in well-defined TQFTs [33–36], further implies that there are also  $(D-k-3), (D-k-2)$ -dimensional excitations. Demanding them to be at least 1-dimensional gives  $k \leq (D-4)$ . Thus  $2 \leq k \leq (D-4)$ , and  $D \geq 6$ . We will provide explicit models for a family of infinite many new non-Abelian topological orders without particles at every  $D \geq 6$  spacetime dimensions.

## 1.1 The model

In this work we will study Non-Abelian self-correcting quantum memory using the following family of non-Abelian TQFTs. We will call them generalized  $\mathbb{D}_8$  theories or the cubic theories.<sup>1</sup> They are described by  $\mathbb{Z}_2$   $m$ -form,  $n$ -form and  $(D-m-n)$ -form gauge theories in  $D$  spacetime dimension, with the topological action

$$\pi \int a_m \cup b_n \cup c_{D-m-n} , \quad (1.1)$$

where  $a_m, b_n, c_{D-m-n}$  are the respective gauge fields. The theory is a non-Abelian TQFT: the fusion rules of the magnetic operators that create holonomy for  $a_m, b_n, c_{D-m-n}$  are non-invertible. For instance, fusing the  $(D-m-1)$  dimensional magnetic operator that creates holonomy of  $a_m$  gives

$$M^{(1)}(M_{D-m-1}) \times M^{(1)}(M_{D-m-1}) = \sum_{\gamma_n, \gamma'_{D-m-n}} W^{(2)}(\gamma_n) W^{(3)}(\gamma'_{D-m-n}) , \quad (1.2)$$

where  $W^2 = (-1)^{\int b_n}$  and  $W^3 = (-1)^{\int c_{D-m-n}}$  are Wilson operators, and the sum is over  $\gamma_n \in H_n(M_{D-m-1}), \gamma'_{D-m-n} \in H_{D-m-n}(M_{D-m-1})$ . The right hand side is a sum of simple objects, and thus the fusion is non-Abelian. For each member in the family, we construct commuting non-Pauli stabilizer lattice models on any triangulated spatial lattice, and in particular on hypercubic lattice. We call such non-Pauli stabilizer models magic stabilizer codes.

We will show that when  $m, n$  obey  $2 \leq m, n \leq D-3, 3 \leq m+n \leq D-2$ , the theory does not have particle excitations. Thus the models provide a family of infinitely many non-Abelian TQFTs without particles in  $D \geq 6$ , such as  $D=6$  and  $m=n=2$ , where the theory describes Abelian loop excitations and non-Abelian membrane excitations. We will argue that the theories provide thermally stable quantum memory.

---

<sup>1</sup>Despite the naming similarity, the theories are not related to Haah's cubic code.

## 1.2 Review of quantum memory at finite temperature for loop toric code

Let us review the basic property of self-correcting quantum memory discussed in Ref. [25] for the example of loop toric code in 4+1d following a Peierls argument. The Hilbert space has physical qubit on each face, and the stabilizer Hamiltonian is

$$H = H_{\text{Gauss}} + H_{\text{Flux}} = - \sum_e \prod_{f \in \partial e} X_f - \sum_c \prod_{f \in \partial c} Z_f . \quad (1.3)$$

The basic excitations are loop excitations created by membrane operators  $\prod X_f$  and  $\prod Z_f$ . Take the error given by electric loop excitation of length  $\ell$  measured in the lattice spacing, which violates  $\ell$  of the Gauss law terms in the Hamiltonian and have energy cost  $E(\ell) = 2\ell\epsilon_0$  where  $\epsilon_0$  is the energy unit of the Hamiltonian. There are  $n(\ell)$  such configuration of length  $\ell$ , and they are suppressed by the Boltzmann factor  $e^{-\beta E(\ell)}$ . Whether large errors are suppressed at low temperature depends on the competition of the this entropy effect and the Boltzmann suppression. The large loop excitation errors are suppressed when

$$e^{-\beta E(\ell)} n(\ell) \ll 1 . \quad (1.4)$$

where  $\beta = 1/(k_B T)$  for temperature  $T$  and Boltzmann constant  $k_B$ . The multiplicity of loops of length  $\ell$  is

$$n(\ell) \sim \text{Polynomial}(\ell) \mu^\ell , \quad (1.5)$$

where  $\mu \sim 6.77$  is the connectivity on 4D hypercubic lattice [37], and only self-avoiding loops are counted by resolving the intersection points without loss of generality. At low temperature, the large loops are exponentially suppressed. The critical temperature below which the errors are suppressed is

$$T_c \sim (2/\log \mu) \epsilon_0 / k_B . \quad (1.6)$$

We will perform a similar analysis for our non-Abelian memory.

The work is organized as follows. In section 2 we discuss a family of infinitely many non-Abelian TQFTs in any dimension. In section 3 we discuss a new example of non-Abelian TQFT in 5+1d with only loops and non-Abelian membrane excitations, and argue that it can provide self-correcting quantum memory at finite temperature. We generalize the thermal stability argument to infinite many models in the family. In section 4 we discuss the results and future directions. There are several appendices. In appendix A we provide an obstruction to non-Abelian TQFT by the absence of lower dimensional excitations. In appendix B we review the definition of cup products on triangulated and hypercube lattices. In appendix C we discuss the CZ,S and Hadamard logical gates in 4D loop toric code.

## 2 Cubic Theory in $D$ dimension as Non-Abelian TQFT

### 2.1 The model

Consider  $\mathbb{Z}_2$   $m$ -form,  $n$ -form and  $(D - m - n)$ -form gauge fields  $a_m, b_n, c_{D-m-n}$ , with the action

$$\pi \int a_m \cup b_n \cup c_{D-m-n} . \quad (2.1)$$

We can write the theory by embedding the gauge fields into  $U(1)$  gauge fields:

$$\frac{1}{\pi^2} \int a_m b_n c_{D-m-n} + \frac{2}{2\pi} \int a_m d\tilde{a}_{D-m-1} + \frac{2}{2\pi} \int b_n d\tilde{b}_{D-n-1} + \frac{2}{2\pi} \int c_{D-m-n} d\tilde{c}_{m+n-1} . \quad (2.2)$$

Examples of the theory are discussed in various literature:

- When  $n = 1, m = 1$ , the gauge fields  $(a_1, b_1, \tilde{c}_1)$  describe the gauge field of  $\mathbb{D}_8$  one-form gauge theory: the equation of motion for  $c_{D-2}$  sets  $d\tilde{c}_1 = \frac{1}{\pi} a_1 b_1$ , which described the extension of  $\mathbb{Z}_2 \times \mathbb{Z}_2$  by  $\mathbb{Z}_2$  with the 2-cocycle given by  $a_1 b_1$ . When  $D = 3$ , the equivalence with the  $\mathbb{D}_8$  gauge theory is discussed in e.g. [38–40].
- When  $m = 2, b = 2$  and  $D = 5$ , this is gauging the  $\mathbb{Z}_2$  0-form symmetry generated by the toric code Walker Wang domain wall.

### 2.2 Hilbert space of TQFT

The equation of motions are

$$\begin{aligned} da_m = 0, \quad db_n = 0, \quad dc_{D-m-n} = 0 \\ d\tilde{a}_{D-m-1} + b_n c_{D-m-n}/\pi = 0, \quad d\tilde{b}_{D-n-1} + a_m c_{D-m-n}/\pi = 0, \quad d\tilde{c}_{m+n-1} + a_m b_n/\pi = 0 . \end{aligned}$$

Thus the Hilbert space of the TQFT on a spatial manifold corresponds can be described by holonomies of  $a_m, b_n, c_{D-m-n}$  subject to the constraints (below we use the normalization that the holonomies are 0, 1 mod 2)

$$a_m \cup b_n = 0, \quad a_m \cup c_{D-m-n} = 0, \quad b_n \cup c_{D-m-n} = 0 . \quad (2.3)$$

We remark that we will describe the TQFT as ground states of a local commuting projector lattice model in section 2.4, where the TQFT Hilbert space is the ground state subspace of the Hamiltonian lattice model.

## 2.3 Operators

The theory has the following well-defined operators:

- The theory has invertible operators generated by the electric Wilson operators (here  $u^{(I)} = (a, b, c)$ ,  $\tilde{u}^{(I)} = (\tilde{a}, \tilde{b}, \tilde{c})$ )
$$W^{(i)} = e^{i \int u^{(I)}} . \quad (2.4)$$

The electric Wilson operators obey  $\mathbb{Z}_2^3$  fusion rule.

- The magnetic operators are

$$\begin{aligned} & e^{i \int_{\Sigma_{D-m-1}} \tilde{a}_{D-m-1+i} \int_{\mathcal{V}_{D-m}} b_n c_{D-m-n} / \pi} \\ & e^{i \int_{\Sigma_{D-n-1}} \tilde{b}_{D-n-1+i} \int_{\mathcal{V}_{D-n}} c_{D-m-n} a_m / \pi} \\ & e^{i \int_{\Sigma_{m+n-1}} \tilde{c}_{m+n-1+i} \int_{\mathcal{V}_{m+n}} a_m b_n / \pi} , \end{aligned} \quad (2.5)$$

where  $\Sigma_k = \partial \mathcal{V}_{k+1}$ . Since in the Hilbert space  $a_m \cup b_n = 0$ ,  $a_m \cup c_{D-m-n} = 0$ ,  $b_n \cup c_{D-m-n} = 0$ , these operators do not depend on  $\mathcal{V}_i$  for  $i = D - m, D - n, m + n$ , respectively [41]. To obtain magnetic operators without  $\mathcal{V}_{k+1}$ , we can put choose a local polarization [42–45], i.e. consider  $\mathcal{V}_{k+1}$  with two boundaries, one with magnetic operators, the other a topological boundary condition. The topological boundary condition can be described by a normal subgroup  $H$  of the bulk gauge group such that the topological action on  $\mathcal{V}_{k+1}$  becomes trivial, i.e. well-defined boundary without gauge anomalies, and a topological action on the boundary for the  $H$  subgroup.

For instance, we can obtain a magnetic operator for  $a_m$  on  $\Sigma_{D-m-1}$  by choosing the other topological boundary to be  $b_n| = 0 = c_{D-m-n}|$ , which gives a magnetic operator decorated with the condensation of the Wilson operators  $W^{(2)}, W^{(3)}$  on  $\Sigma_{D-m-1}$  that imposes the projection to  $b_n| = 0, c_{D-m-n}| = 0$  [46]. We will call such magnetic operator  $M^{(1)}$ , and similarly define  $M^{(2)}, M^{(3)}$  using the Dirichlet boundary conditions of  $(a_m, c_{D-m-n}), (a_m, b_n)$ , respectively.

From the condensate of Wilson operators, one can derive the non-Abelian fusion rules (see also [41])

$$\begin{aligned} M^{(I)} \times W^{(J)} &= M^{(I)} , I \neq J \\ M^{(I)} \times M^{(I)} &= \sum W^{(J)}(\gamma) W^{(K)}(\gamma') , I, J, K \text{ distinct} . \end{aligned} \quad (2.6)$$

- Gauged symmetry-protected topological (SPT) operators [47–49, 41, 50]  $H^*(B^m \mathbb{Z}_2 \times B^n \mathbb{Z}_2 \times B^{D-m-n} \mathbb{Z}_2, U(1))$ . The closed gauged SPT operators  $\int a_m b_n, \int a_m c_{D-m-n}, \int b_n c_{D-m-n}$  are trivial. There are following nontrivial gauged SPT operators:

$$V^{12} = e^{i \int a_m d b_n / (2\pi)} , \quad V^{23} = e^{i \int b_n d c_{D-m-n} / (2\pi)} , \quad V^{13} = e^{i \int a_m d c_{D-m-n} / (2\pi)} . \quad (2.7)$$



- “Mixed” operators that involve the electric and the magnetic operators:

$$\begin{aligned}
& e^{i \int_{\partial M_{D-n+m}} a_m \tilde{b}_{D-n-1/\pi+i} \int_{M_{D-n+m}} a_m^2 c_{D-m-n}/\pi^2} \\
& e^{i \int_{\partial M_{D-m+n}} b_n \tilde{a}_{D-m-1/\pi+i} \int_{M_{D-m+n}} b_n^2 c_{D-m-n}/\pi^2} \\
& e^{i \int_{\partial M_{m+2n}} b_n \tilde{c}_{m+n-1/\pi+i} \int_{M_{m+2n}} b_n^2 a_m/\pi^2} \\
& e^{i \int_{\partial M_{2D-m-2n}} c_{D-m-n} \tilde{b}_{D-n-1/\pi+i} \int_{M_{2D-m-2n}} c_{D-m-n}^2 a_m/\pi^2} \\
& e^{i \int_{\partial M_{2m+n}} a_m \tilde{c}_{m+n-1/\pi+i} \int_{M_{2m+n}} a_m^2 b_n/\pi^2} \\
& e^{i \int_{\partial M_{2D-m-2n}} c_{D-m-n} \tilde{a}_{D-n-1/\pi+i} \int_{M_{2D-m-2n}} c_{D-m-n}^2 b_n/\pi^2} .
\end{aligned} \tag{2.8}$$

As in the magnetic operators, these operators do not depend on the bulk. To define operators without using the bulk, we can choose a local polarization by putting the operator on one boundary and a topological boundary condition on the other boundary. For instance, in the first operator we can impose the Dirichlet boundary conditions for  $a_m, c_{D-m-n}$ , and similar for the other operators. Let us call the resulting operators on the boundary  $\mathcal{D}^{12}, \mathcal{D}^{21}, \mathcal{D}^{23}, \mathcal{D}^{32}, \mathcal{D}^{13}, \mathcal{D}^{31}$ . Due to the condensate from the topological boundary conditions, the operators  $\mathcal{D}^{ij}$  are non-invertible.

The operators act on the Wilson and magnetic operators. For instance, when the Wilson operator  $W^{(2)}$  intersects  $\mathcal{D}^{12}$ , it creates holonomy for  $\tilde{b}_{D-n-1}$ , and results in additional Wilson operator  $W^{(1)}$ . On the other hand, when the magnetic operator  $M^{(1)}$  intersects  $\mathcal{D}^{12}$ , the projectors for  $W^{(1)}$  annihilate the magnetic operator, and similarly for  $M^{(3)}$ . In other words, the magnetic operators  $M^{(1)}, M^{(3)}$  cannot intersect with or terminate at  $\mathcal{D}^{12}$ :

$$\mathcal{D}^{12} : \quad W^{(1)} \rightarrow W^{(1)}, \quad W^{(2)} \rightarrow W^{(1)}W^{(2)}, \quad M^{(1)} \rightarrow 0, \quad M^{(3)} \rightarrow 0 . \tag{2.9}$$

## 2.4 Lattice model

Let us construct a local commuting non-Pauli stabilizer Hamiltonian for the Cubic theory in  $D$  spacetime dimension. We can begin by constructing a Hamiltonian model for the SPT phase with  $\mathbb{Z}_2$   $(m-1)$ -form symmetry,  $(n-1)$ -form symmetry, and  $(D-m-n-1)$ -form symmetry, and then gauge these symmetries minimally.

**SPT Hamiltonian** A lattice Hamiltonian model for the SPT phase with the cocycle<sup>2</sup>

$$\phi_D(a_m, b_n, c_{D-m-n}) = \pi a_m \cup b_n \cup c_{D-m-n} \tag{2.10}$$

---

<sup>2</sup>Properties of cup products on triangulated or hypercubic lattice are reviewed in e.g. [51–53, 22] (see also appendix B).

can be constructed using the method in e.g. [54, 55]. We introduce a qubit on each  $(m-1)$ -simplex,  $(n-1)$ -simplex and  $(D-m-n-1)$ -simplex, acted by Pauli operators  $X^{0,i}, Y^{0,i}, Z^{0,i}$ . Denote  $\lambda^i = (1 - Z^{0,i})/2$ . The entangler of the SPT wavefunction is

$$(-1)^{\int \lambda^1 \cup d\lambda^2 \cup d\lambda^3}, \quad (2.11)$$

where the integral is over the space. The SPT Hamiltonian is given by conjugating the paramagnet  $H^0 = -\sum X^{0,1} - \sum X^{0,2} - \sum X^{0,3}$  by the entangler:

$$\begin{aligned} H_{\text{SPT}} = & - \sum_{s_{m-1}} X_{s_{m-1}}^{0,1} (-1)^{\int \tilde{s}_{m-1} \cup d\lambda^2 \cup d\lambda^3} - \sum_{s_{n-1}} X_{s_{n-1}}^{0,2} (-1)^{\int \tilde{d}\lambda^1 \cup \tilde{s}_{n-1} \cup d\lambda^3} \\ & - \sum_{s_{D-m-n-1}} X_{s_{D-m-n-1}}^{0,3} (-1)^{\int d\lambda^1 \cup d\lambda^2 \cup \tilde{s}_{D-m-n-1}}, \end{aligned} \quad (2.12)$$

where  $s_n$  are  $n$ -simplices, and  $\tilde{s}_n$  is the  $n$ -cochain that takes value 1 on  $s_n$  and zero otherwise.

**Cubic Theory Hamiltonian** We can gauge the symmetries following the method in e.g. [56–58] by introducing gauge fields qubits on each  $m, n, (D-m-n)$  simplicies, acted by the Pauli operators  $X^i, Y^i, Z^i$  with  $i = 1, 2, 3$  for the three types of qubits. Denote  $a_m = (1 - Z^1)/2$ ,  $b_n = (1 - Z^2)/2$ ,  $c_{D-m-n} = (1 - Z^3)/2$ . After gauge-fixing to remove the original qubits, the Hamiltonian of the gauged theory is

$$\begin{aligned} H_{\text{Cubic}} = & H_{\text{Gauss}} + H_{\text{Flux}}, \\ H_{\text{Gauss}} = & - \sum_{s_{m-1}} \left( \prod_{\partial s_m \subset s_{m-1}} X_{s_m}^1 \right) (-1)^{\int \tilde{s}_{m-1} \cup b_n \cup c_{D-m-n}} \\ & - \sum_{s_{n-1}} \left( \prod_{\partial s_n \subset s_{n-1}} X_{s_{n-1}}^2 \right) (-1)^{\int a_m \cup \tilde{s}_{n-1} \cup c_{D-m-n}} \\ & - \sum_{s_{D-m-n-1}} \left( \prod_{\partial s_{D-m-n} \subset s_{D-m-n-1}} X_{s_{D-m-n}}^3 \right) (-1)^{\int a_m \cup b_n \cup \tilde{s}_{D-m-n-1}}, \end{aligned} \quad (2.13)$$

where  $s_n$  are  $n$ -simplices on the lattice, and the flux terms  $H_{\text{flux}}$  are

$$H_{\text{flux}} = - \sum_{s_{m+1}} \left( \prod_{s_m \in \partial s_{m+1}} Z_{s_m}^1 \right) - \sum_{s_{n+1}} \left( \prod_{s_n \in \partial s_{n+1}} Z_{s_n}^2 \right) - \sum_{s_{D-m-n+1}} \left( \prod_{s_{D-m-n} \in \partial s_{D-m-n+1}} Z_{s_{D-m-n}}^3 \right). \quad (2.14)$$

The Gauss law Hamiltonian  $H_{\text{Gauss}}$  consists of products of  $X^i$  and  $CZ^{jk}$  for distinct  $j, k \neq i$ .

#### 2.4.1 Commuting non-Pauli stabilizer lattice model

We note that the Gauss law terms  $H_{\text{Gauss}}$  only commute among themselves on the zero flux sector. To make them exactly commute, we can modify the Gauss law term by multiplying

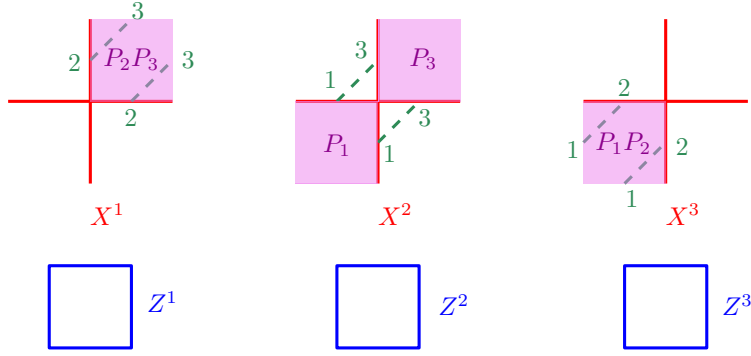


Figure 1: Non-Pauli stabilizer model for  $D = 3, m = n = 1$  cubic theory, which is equivalent to ordinary  $\mathbb{D}_8$  gauge theory in 2+1d. Here  $P_i(f) = \frac{1 + \prod_{e \in \partial f} Z_e^i}{2}$  is the projector to zero flux on face  $f$ . The dashed line with endpoints  $i, j$  is the operator  $CZ^{i,j}$  on the qubits  $i, j$  on the edges connected by the line. The upper figures can multiply with addition flux projectors and still maintain the commuting property.

them with projectors to zero fluxes. We note that the flux projectors commute with each term in  $H_{\text{Gauss}}$ , and thus the ordering of the projectors do not matter. This gives commuting Gauss law Hamiltonian:

$$\begin{aligned}
& H'_{\text{Gauss}} \\
&= - \sum_{s_{m-1}} \left( \prod_{\partial s_m \subset s_{m-1}} X_{s_m}^1 \right) (-1)^{\int \tilde{s}_{m-1} \cup b_n \cup c_{D-m-n}} \\
&\quad \prod_{s'_{n-1}} \left( \frac{1 + (-1)^{\int \tilde{s}_{m-1} \cup \tilde{s}'_{n-1} \cup dc_{D-m-n}}}{2} \right) \prod_{s''_{D-m-n-1}} \left( \frac{1 + (-1)^{\int \tilde{s}_{m-1} \cup db_n \cup \tilde{s}''_{D-m-n-1}}}{2} \right) \\
&- \sum_{s_{n-1}} \left( \prod_{\partial s_n \subset s_{n-1}} X_{s_{n-1}}^2 \right) (-1)^{\int a_m \cup \tilde{s}_{n-1} \cup c_{D-m-n}} \\
&\quad \prod_{s'_{m-1}} \left( \frac{1 + (-1)^{\int \tilde{s}'_{m-1} \cup \tilde{s}_{n-1} \cup dc_{D-m-n}}}{2} \right) \prod_{s''_{D-m-n-1}} \left( \frac{1 + (-1)^{\int da_m \cup \tilde{s}_{n-1} \cup \tilde{s}''_{D-m-n-1}}}{2} \right) \\
&- \sum_{s_{D-m-n-1}} \left( \prod_{\partial s_{D-m-n} \subset s_{D-m-n-1}} X_{s_{D-m-n}}^3 \right) (-1)^{\int a_m \cup b_n \cup \tilde{s}_{D-m-n-1}} \\
&\quad \prod_{s'_{m-1}} \left( \frac{1 + (-1)^{\int \tilde{s}'_{m-1} \cup db_n \cup \tilde{s}_{D-m-n-1}}}{2} \right) \prod_{s''_{n-1}} \left( \frac{1 + (-1)^{\int da_m \cup \tilde{s}''_{n-1} \cup \tilde{s}_{D-m-n-1}}}{2} \right). \quad (2.15)
\end{aligned}$$

**Locality of Hamiltonian** Each term in the Hamiltonian (2.15) is local. This is because on hypercubic lattice, for a given simplex  $s_k$  and integers  $l, l', \tilde{s}_k \cup \tilde{s}_l \neq 0, \tilde{s}_{l'} \cup \tilde{s}_k \neq 0$  for

finite number of simplices  $s_l, s_{l'}$  independent of the system size. More explicitly, the number of  $s_l$  is given by choosing  $l$  positive spatial directions in the complementary  $(D - k - 1)$  spatial directions, which is  $\binom{D - k - 1}{l}$ . Similarly, the number of  $s_{l'}$  is  $\binom{D - k - 1}{l'}$ . For example, if  $l = D - k - 1$  or  $l' = D - k - 1$ , there is a unique choice of  $s_l$  or  $s_{l'}$ .

**Local commuting non-Pauli stabilizer Hamiltonian** The modified Hamiltonian

$$H'_{\text{Cubic}} = H'_{\text{Gauss}} + H_{\text{Flux}} \quad (2.16)$$

is a sum of local commuting terms and has the same ground states as the Hamiltonian  $H_{\text{Cubic}}$ . We remark that the cup product expression allows us to define the model on any lattice that admits a triangulation. For example, when  $D = 3, m = n = 1$ , the model is illustrated in figure 1. The lattice model defines a non-Pauli stabilizer code describing non-Abelian topological orders, and we will call it magic stabilizer code.

**Excitations** Since the Hamiltonian is a sum of local commuting terms, we can analyze the errors for each term independently, just as in the Calderbank-Shor-Steane (CSS) codes.

The basic electric excitations are given by violations of the Gauss law term by  $1 - (-1) = 2$  but not the flux term. The basic magnetic excitations are given by violations of the flux terms by  $1 - (-1) = 2$  and violation of the Gauss law terms by  $0 - (-1) = 1$ .

## 2.5 Cubic theories without particles

Let us consider the class of cubic theories that do not have particles. In other words, all gauge fields  $a, b, c, \tilde{a}, \tilde{b}, \tilde{c}$  have degree greater or equal 2. This requires

$$m \geq 2, \quad n \geq 2, \quad D - m - n \geq 2, \quad D - m - 1 \geq 2, \quad D - n - 1 \geq 2, \quad m + n - 1 \geq 2. \quad (2.17)$$

These conditions simplify to

$$2 \leq m \leq D - 3, \quad 2 \leq n \leq D - 3, \quad 3 \leq m + n \leq D - 2. \quad (2.18)$$

The first two equations imply  $4 \leq m + n \leq 2D - 6$ , and together with the last inequality gives  $D \geq 6$ . The condition on spacetime dimension  $D$  is consistent with the no-go theorem for non-Abelian TQFTs without particles. The equality is attained with  $D = 6, m = n = 2$ . For every spacetime dimension above 6, there is a non-Abelian TQFT without particles given by the cubic theory with  $m = n = 2$ .

As a consistency check, we note that in theories without particles, since the electric excitations obey Abelian fusion rule and magnetic excitations obey non-Abelian fusion rules, the dimensions of the magnetic excitations must be strictly greater than the minimal dimension of the electric excitations due to the constraint discussed in appendix A (see also [31, 32]):

$$\begin{aligned}
D - m - 1 &> \min(m, n, D - m - n) \\
D - n - 1 &> \min(m, n, D - m - n) \\
m + n - 1 &> \min(m, n, D - m - n) .
\end{aligned} \tag{2.19}$$

In such case, we can use electric excitations to form condensate whose dimension is one less than that of the magnetic excitations. Since there are condensates of all dimensions down to the dimension of the electric excitation itself which obeys Abelian fusion rules, the condition in appendix A follows from (2.19). On the other hand, we can reproduce the conditions (2.19) from the inequalities in (2.18) for the cubic theories without particles:

- The first two inequalities of (2.19) are related by  $m \leftrightarrow n$ , so without loss of generality we can consider the first one of them. Suppose the minimum on the right hand side is  $(D - m - n)$  (including the case when the minimum is degenerate), then  $(D - m - 1) > (D - m - n)$  follows from  $n \geq 2$  in (2.18). Suppose the minimum on the right hand side is instead  $m$  or  $n$ , i.e.  $m < n$ ,  $(D - m - n)$  or  $n < m$ ,  $(D - m - n)$ , then  $(D - m - 1) > (m + n - 1) > m$  or  $(D - m - 1) > (n + n - 1) > n$  due to  $n \geq 2$  from (2.18).
- In the last inequality of (2.19), suppose the minimum on the right hand side is  $m$  or  $n$  (including the case when the minimum is degenerate), then the inequality follows from  $n \geq 2$  or  $m \geq 2$  in (2.18). Suppose the minimum on the right hand side is instead  $(D - m - n) < m, n$ , which implies  $2(D - m - n) < (m + n)$ , i.e.  $(m + n) > 2D/3$ , then  $2(m + n) > 4D/3 > D + 1$  where the second inequality follows from  $D \geq 6$  in (2.18), and this then implies the desired inequality  $(m + n - 1) > (D - m - n)$ .

Thus the theories without particles have the properties that the lowest dimensional excitations obey Abelian fusion rule, in agreement with constraint on excitations with non-Abelian fusion rules (see e.g. appendix A).

## 2.6 Cubic theory from compactification of generalized color code

The cubic theory in  $D$  spacetime dimension can be obtained from twisted compactification of a generalized color code theory in  $(D + 1)$  spacetime dimension [30, 59], where the generalized

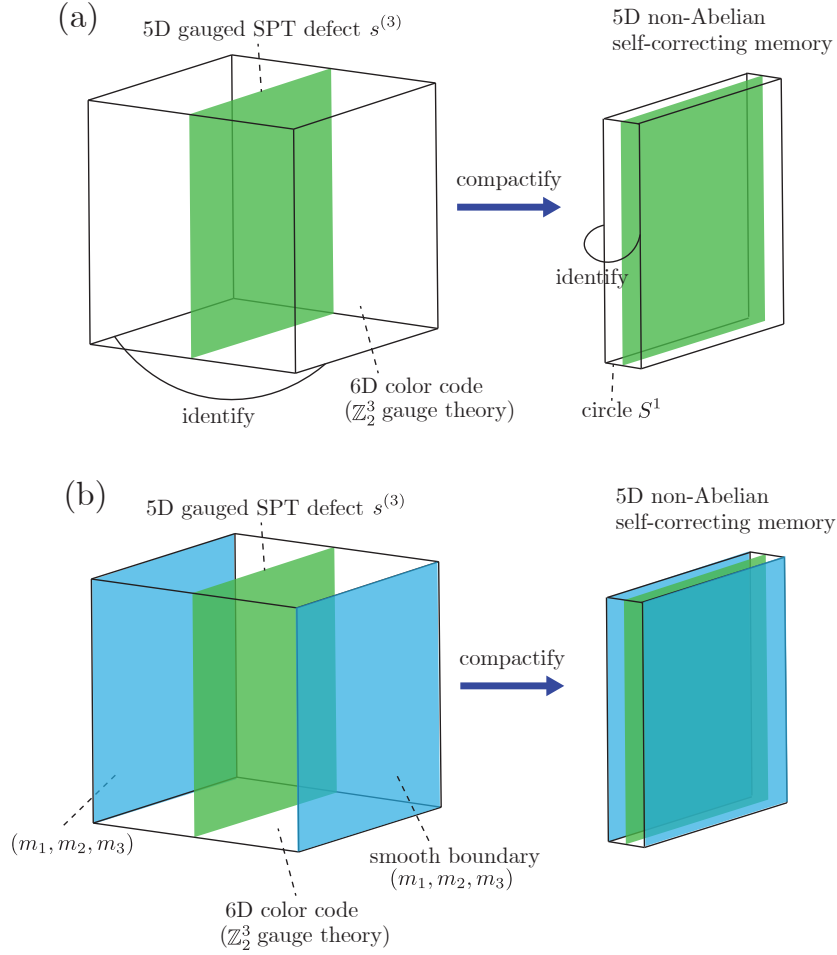


Figure 2: Non-Abelian self-correcting memory from (a) compactification of color code on a circle with gauged SPT defect inserted, and (b) reduction on an interval with  $m$ -condensed boundaries (i.e. Neumann boundary conditions for the higher-form  $\mathbb{Z}_2$  gauge fields) on two ends and the gauged SPT defect inserted in the middle.

color code theory is equivalent to decoupled  $\mathbb{Z}_2$   $m$ -form gauge theory,  $\mathbb{Z}_2$   $n$ -form gauge theory and  $\mathbb{Z}_2$   $(D - m - n)$ -form gauge theory.

The  $(D + 1)$ -dimensional theory can be described by three copies of  $\mathbb{Z}_2$  toric code with qubits on spatial  $m$ -simplices,  $n$ -simplices and  $(D - m - n)$ -simplices, respectively. We note that the three types of simplices meet at a point in the  $D$ -dimensional space. It is equivalent to a single copy of generalized color code up to a constant-depth local quantum circuit (see e.g. [59, 60, 30]). For example, the  $D = 6, m = 2, n = 4$  case corresponds to the 6D color code self-correcting memory described in Ref. [30], which gives rise to our non-Abelian self-correcting memory in five spatial dimensions after the twisted compactification process.

The  $(D + 1)$  dimensional theory has a  $\mathbb{Z}_2$  0-form symmetry generated by gauged SPT defect (denoted by  $s^{(3)}$ ) [47–49, 41, 50] given by domain wall decorated with the topological action (2.1). If the space is  $S^m \times S^n \times S^{D-m-n}$ , the  $\mathbb{Z}_2$  0-form symmetry acts as a constant-depth circuit composed of the product of CCZ gates on the triplet of qubits in three copies of toric codes respectively, which is dual to the transversal  $T$  gate in the generalized color code [59]. The corresponding symmetry operator in the TQFT can be expressed as:

$$\mathcal{D}_{s^{(3)}}(M_{D+1}) = \exp \left( \pi i \int_{M_{D+1}} a_m \cup b_n \cup c_{D-m-n} \right), \quad (2.20)$$

where for the  $D = 3, m = 1, n = 1$  case the correspondence to the CCZ gates in three copies of 3D toric codes has been discussed in Ref. [50] and the correspondence to the transversal  $T$  gates in the 3D color code can be found in Ref. [61].

We note that when a magnetic defect of one gauge field pierces the domain wall  $s^{(3)}$ , it forms a junction with the domain wall that has the non-Abelian magnetic defect in the cubic theory, whose fusion produces the Wilson operators for the other two  $\mathbb{Z}_2$  gauge fields. This gives an operator-value associator similar to the junction discussed in section 2.3 of [62].

The twisted compactification of the  $(D + 1)$ -dimensional theory to  $D$  spacetime dimensions is given by turning on holonomy of this  $\mathbb{Z}_2$  0-form symmetry along the internal circle direction, i.e. placing the domain wall at a point on the circle, and we keep only the zero modes of the gauge fields  $a_m, b_n, c_{D-m-n}$  that do not wind around the circle.<sup>3</sup> The holonomy introduce the action

$$\pi \int a_m \cup b_n \cup c_{D-m-n} \cup (d\theta/2\pi), \quad (2.21)$$

where  $\theta \sim \theta + 2\pi$  is the coordinate of the circle, and this corresponds to the background gauge field  $d\theta/2\pi$  for the  $\mathbb{Z}_2$  0-form symmetry. Integrating over the circle direction gives the topological action (2.1). Alternatively, we can reduce the  $(D + 1)$ -dimensional theory on an interval with Neumann boundary condition for the gauge fields and the  $\mathbb{Z}_2$  domain wall in the middle. The Neumann boundary conditions for the gauge fields correspond to the  $m$ -condensed or smooth boundaries. See Fig. 2 for an illustration.

We remark that similar twisted dimensional reduction for twisted gauge theory in  $D = 3$  is discussed in [40].

---

<sup>3</sup>The winding modes will give additional  $(m - 1)$ -form,  $(n - 1)$ -form and  $(D - m - n - 1)$ -form gauge fields  $\int_{S^1} a_m, \int_{S^1} b_n, \int_{S^1} c_{D-m-n}$ .

### 3 Self-Correcting Cubic Theory of Strings and Membranes

In the following, we will focus on the cubic theory with  $m = n = 2$ ,  $D = 6$ . This is a non-Abelian TQFT in 5+1d with strings and membranes. The strings obey Abelian fusion rule [31,32], while the membranes are non-Abelian.

#### 3.1 TQFT Hilbert space

The equation of motion implies

$$a_2 \cup b_2 = 0, \quad a_2 \cup c_2 = 0, \quad b_2 \cup c_2 = 0. \quad (3.1)$$

The Hilbert space is described by different holonomies of the two-form  $\mathbb{Z}_2$  gauge fields  $a_2, b_2, c_2$  subject to the above constraint.

For instance, suppose the space is  $S^2 \times S^2 \times S^1$ . Denote the holonomies on the two  $S^2$ s by the three-component vectors  $\vec{n}_i = (n_i^a, n_i^b, n_i^c)$  with  $n_i^a = 0, 1 \pmod 2$  is the holonomy of  $a_2$  on the  $i$ th  $S^2$ , the constraint is

$$\vec{n}_1 \times \vec{n}_2 = 0 \pmod 2. \quad (3.2)$$

There are 22 solutions, thus the Hilbert space of the TQFT on  $S^2 \times S^2 \times S^1$  has dimension 22.

#### 3.2 Operators

There are Wilson surface operators

$$W^{(1)} = e^{i \int a_2}, \quad W^{(2)} = e^{i \int b_2}, \quad W^{(3)} = e^{i \int c_2}. \quad (3.3)$$

The integral is over the support of the Wilson surface, given by 2-cycles  $M_2$ . The Wilson surface operators obey  $\mathbb{Z}_2^3$  fusion rule. Under union of surfaces, the Wilson operators satisfy  $W^{(i)}(M_2) \times W^{(i)}(M'_2) = W^{(i)}(M_2 + M'_2)$  for any two 2-cycles  $M_2, M'_2$ . On the lattice, they are described by product of  $Z^i$  for each  $i$ . The Wilson surface operators correspond to string excitations, and they obey  $\mathbb{Z}_2^3$  fusion rules.

There are magnetic volume operators

$$M^{(1)} = e^{i \int \tilde{a}_3 + i \int b_2 c_2 / \pi}, \quad M^{(2)} = e^{i \int \tilde{b}_3 + i \int a_2 c_2 / \pi}, \quad M^{(3)} = e^{i \int \tilde{c}_3 + i \int a_2 b_2 / \pi}. \quad (3.4)$$

The integral is over the support of the volume operators, given by 3-cycles  $M_3$ .



### 3.3 Commuting non-Pauli stabilizer lattice Hamiltonian model

On each face we introduce three types of qubits for  $a_2, b_2, c_2$ , acted by Pauli operators  $X^i, Y^i, Z^i$ . Denote  $a_2 = (1 - Z^1)/2, b_2 = (1 - Z^2)/2, c_2 = (1 - Z^3)/2$ . The model is

$$\begin{aligned}
H = & - \sum_e \left( \prod_{\partial f \supseteq e} X_f^1 \right) (-1)^{\int \tilde{e} \cup b_2 \cup c_2} \prod_{e'} \left( \frac{1 + (-1)^{\int \tilde{e} \cup \tilde{e}' \cup dc_2}}{2} \right) \prod_{e''} \left( \frac{1 + (-1)^{\int \tilde{e} \cup db_2 \cup \tilde{e}''}}{2} \right) \\
& - \sum_e \left( \prod_{\partial f \supseteq e} X_f^2 \right) (-1)^{\int a_2 \cup \tilde{e} \cup c_2} \prod_{e'} \left( \frac{1 + (-1)^{\int \tilde{e}' \cup \tilde{e} \cup dc_2}}{2} \right) \prod_{e''} \left( \frac{1 + (-1)^{\int da_2 \cup \tilde{e} \cup \tilde{e}''}}{2} \right) \\
& - \sum_e \left( \prod_{\partial f \supseteq e} X_f^3 \right) (-1)^{\int a_2 \cup b_2 \cup \tilde{e}} \prod_{e'} \left( \frac{1 + (-1)^{\int \tilde{e}' \cup db_2 \cup \tilde{e}'}}{2} \right) \prod_{e''} \left( \frac{1 + (-1)^{\int da_2 \cup \tilde{e}'' \cup \tilde{e}}}{2} \right) \\
& + H_{\text{Flux}} .
\end{aligned} \tag{3.5}$$

For instance, on the 5D space with coordinate  $(x, y, z, u, v)$ , the first term without the projector on the edge  $(x, y, z, u, v) = (0, 0, 0, 0, 0)$  to  $(1, 0, 0, 0, 0)$  in the  $x$  direction is given by product of  $X_f^1$  on the 8 faces that span respectively the  $\hat{x} \times (\pm \hat{y}), \hat{x} \times (\pm \hat{z}), \hat{x} \times (\pm \hat{u}), \hat{x} \times (\pm \hat{v})$  directions, where  $\hat{x}$  denotes the unit vector in the  $x$  direction. The  $(-1)^{\int \tilde{e} \cup b_2 \cup c_2}$  is given by  $CZ_{f, f'}$  of the physical qubits that are acted by the Pauli operators  $X_f^2, X_{f'}^3$  on the following pair of faces:

- $f = (x = 1, \text{Square}_{y=0, z=0}, u = v = 0)$  and  $f' = (x = 1, y = 1, z = 1, \text{Square}_{u=0, v=0})$ , where  $\text{Square}_{y=0, z=0}$  is the unit area square on the  $y, z$ -plane with four vertices  $(y, z) = (0, 0), (0, 1), (1, 0), (1, 1)$ . We note that the face  $f$  meet the edge  $(0 \leq x \leq 1, y = z = u = v = 0)$  at a single point  $(x = 1, y = z = u = v = 0)$ , the face  $f'$  does not meet this edge, and the faces  $f, f'$  meet at a single point  $(x = 1, y = 1, z = 1, u = v = 0)$ .
- The other pairs are permutations of  $y, z, u, v$ , with total  $\binom{4}{2} = 6$  pairs of  $(f, f')$  in total.

The projectors are product of the zero flux projectors  $(1 + \prod_{f'' \in \partial c} Z_{f''}^2)/2, (1 + \prod_{f''' \in \partial c'} Z_{f'''}^3)/2$  over the neighboring cubes  $c, c'$ .

#### 3.3.1 Operators on the lattice

**Wilson membrane operators** On the lattice, there are Wilson membrane operators given by product  $\prod Z_f^i$  over each small faces on the membrane. On non-contractible 2-cycles they give rise to nontrivial logical operators.

**Magnetic volume operators** There are also magnetic volume operators described by product of  $X^i$  together with projectors for each  $i$ . The projector is product  $(1 + Z^j)(1 + Z^k)$  on non-contractible 2-cycles in the volume for distinct  $j, k \neq i$  to preserve the holonomy condition (3.1), i.e. project out the states that will violate the condition after applying  $X^i$ . On the 5-dimensional hypercubic spatial lattice, the magnetic operators on 3-cycle  $M_3$  are

$$M^{(i)}(M_3) = P \left[ X^i(M_3^\vee) \prod_{f, f' \subset M_3} (1 + Z_f^j) (1 + Z_{f'}^k) \right] P \quad (3.6)$$

for distinct  $j, k \neq i$ , where  $M_3^\vee$  is the 2-cycle that intersects with  $M_3$  at a point in space, and  $X^i(M_3^\vee)$  is the product of  $X^i$  over faces crossing  $M_3^\vee$ . The term  $(1 + Z_f^j) (1 + Z_{f'}^k)$  are projectors for  $Z^j, Z^k$  support at  $M_3$ . The projectors enforce the condition (3.1) evaluated on  $M_3^\vee \times M_2, M_3^\vee \times M'_2$  when the holonomy of the  $i$ th gauge field is changed on  $M_3^\vee$  ( $i = a, b, c$ ). The operator denotes the projector onto the ground state subspace, i.e. the product of projectors for all local stabilizers.

As a consequence of the projector, the magnetic operators are non-invertible, but obey the fusion rule

$$M^{(i)}(M_3) \times M^{(i)}(M_3) = \sum_{M_2, M'_2 \in H_2(M_3)} W^{(j)}(M_2) W^{(k)}(M'_2), \quad (3.7)$$

for distinct  $j, k \neq i$ . Thus the magnetic volume operators describe non-Abelian membrane excitations.

### 3.3.2 Code distance

We remark that on a hypercubic lattice with linear size  $L$  in each direction, the minimal logical operator is given by Wilson membrane operators of size  $L^2$ . The errors created by smaller size operators correspond to excited states. Thus the code distance is  $d = O(L^2) = O(N^{\frac{2}{5}})$ , where  $N = O(L^5)$  represents the total number of qubits.

## 3.4 Non-Abelian braiding of magnetic operators

**Two-membrane braiding gives 0** The magnetic operators obey non-Abelian braiding following the method of [41]. The braiding can be derived from the commutator of the non-invertible operators (3.6). Consider the correlation function of two different magnetic operators

$$\langle M^{(1)}(V_3) M^{(2)}(V'_3) \rangle. \quad (3.8)$$

The equation of motion for  $\tilde{a}_3, \tilde{b}_3$  sets  $da_2 = -\pi\delta(V_3)^\perp$ ,  $db_2 = -\pi\delta(V'_3)^\perp$ , where  $\delta(V_3)^\perp$  is a delta function 3-form that restricts integrals to  $V_3$ . For  $V_3 = \partial V_4, V'_3 = \partial V'_4$  this reduces to  $a_2 = -\pi\delta(V_4)^\perp, b_2 = -\pi\delta(V'_4)^\perp$ . We are left with

$$e^{i\int c_2\delta(V_4)^\perp\delta(V'_4)^\perp} . \quad (3.9)$$

The equation of motion for  $c_2$  sets  $d\tilde{c}_3 = \pi\delta(V_4)^\perp\delta(V'_4)^\perp$ . For non-exact  $\delta(V_4)^\perp\delta(V'_4)^\perp$  the equation does not have a solution, and thus the correlation function is zero. Another way to see the correlation function is zero is by performing path integral over  $\mathbb{Z}_2$  gauge field  $c_2$ , whose possible holonomy is  $0, \pi \pmod{2\pi}$ : for the configuration where  $\int c_2\delta(V_4)^\perp\delta(V'_4)^\perp = 0, \pi$ , the correlation function is

$$e^{0i} + e^{\pi i} = 0 . \quad (3.10)$$

Such vanishing correlation function indicates the magnetic operators are non-Abelian. This generalizes the vanishing Hopf braiding of two non-Abelian particles in 2+1d  $\mathbb{D}_8$  gauge theory (see e.g. [39]). The above computation indicates that there are two braiding channels.

In the lattice model on periodic space of  $T^5$  topology, consider the commutator of the magnetic operators  $M^{(1)}(T_{1,2,3}^3), M^{(2)}(T_{1,4,5}^3)$  supported on two 3-tori with subscripts labelling the coordinates, where

$$\begin{aligned} M^{(1)}(T_{1,2,3}^3) &= P \left[ X^1(T_{1,2,3}^{3\vee}) \prod_{f,f' \subset T_{1,2,3}^3} (1 + Z_f^2) (1 + Z_{f'}^3) \right] P \\ &= P \left[ X^1(T_{1,2,3}^{3\vee}) \prod_{f,f' \subset T_{1,2,3}^3} (1 + Z_f^2) (1 + Z_{f'}^3) \cdot \frac{1 + Z^2(T_{2,3}^2)}{2} \right] P \\ M^{(2)}(T_{1,4,5}^3) &= P \left[ X^1(T_{1,4,5}^{3\vee}) \prod_{f,f' \subset T_{1,4,5}^3} (1 + Z_f^2) (1 + Z_{f'}^3) \right] P , \end{aligned} \quad (3.11)$$

where  $Z^2(T_{2,3}^2)$  is the product of  $Z_f^2$  over the 2-torus  $T_{2,3}^2$ . From the above expressions we find

$$M^{(1)}(T_{1,2,3}^3)M^{(2)}(T_{1,4,5}^3) = M^{(1)}(T_{1,2,3}^3)M^{(2)}(T_{1,4,5}^3) \cdot \frac{1 - Z^2(T_{2,3}^2)}{2} \quad (3.12)$$

due to the anti-commutation relation between  $Z^2(T_{2,3}^2)$  and  $X^1(T_{1,4,5}^{3\vee})$ . Meanwhile we have

$$M^{(1)}(T_{1,2,3}^3)M^{(2)}(T_{1,4,5}^3) = \frac{1 + Z^2(T_{2,3}^2)}{2} M^{(1)}(T_{1,2,3}^3)M^{(2)}(T_{1,4,5}^3) . \quad (3.13)$$

The braiding can then be obtained as

$$M^{(1)}(T_{1,2,3}^3)M^{(2)}(T_{1,4,5}^3)M^{(1)}(T_{1,2,3}^3)M^{(2)}(T_{1,4,5}^3) = 0 , \quad (3.14)$$

which follows from  $(1 - Z^2(T_{2,3}^2))(1 + Z^2(T_{2,3}^2)) = 0$ , i.e.  $M^{(1)}(T_{1,2,3}^3)M^{(2)}(T_{1,4,5}^3)$  and  $M^{(2)}(T_{1,4,5}^3)M^{(1)}(T_{1,2,3}^3)$  have orthogonal projectors.

**“Borromean rings” braiding of membranes** If we include additional magnetic operator  $M^{(3)}(V_3'')$ , i.e. correlation function of  $M^{(1)}(V_3), M^{(2)}(V_3'), M^{(3)}(V_3'')$ , the new magnetic operator sources the holonomy of  $c_2 = -\pi\delta(V_4'')$  with  $\partial V_4'' = V_3''$ , thus the three magnetic operators have the correlation function

$$(-1)^{\int \delta(V_4) \delta(V_4') \delta(V_4'')} . \quad (3.15)$$

The correlation gives  $(-1)$  for the three volume operators arranged in analogue of Borromean rings. The discussion is similar to the  $D = 3, m = n = 1$  case in [63].

### 3.5 Self-correcting quantum memory

Let us analyze the self-correcting property for the model on 5-dimensional hypercubic spatial lattice. The Hamiltonian model in section 2.4 with  $m = n = 2, D = 6$  has Gauss law term for each edge and flux term for each cube, and each face has 3 types of qubits for  $a, b, c$ .

Since we have a commuting (non-Pauli) stabilizer models in Eq. (2.16), the errors inducing the loop and membrane excitations can be decoupled and corrected independently, similar to the 4D self-correcting toric-code case where the e-excitations induced by the Z-type errors and m-excitations induced by the X-type errors can be corrected independently. Thus, we will apply a similar analysis using a Peierls argument as in Ref. [25] for the 4D toric code.

We consider the quantum memory being coupled to a thermal bath with temperature  $T$  and focus on the thermal noise since its not correctable for usual topological memories without self-correction capability.

**Errors inducing loop excitations** We first discuss correction of the errors inducing loop excitations. The unit-time probability for creation or survival of a small loop excitation on a plaquette, i.e. violating the Gauss term on the 4 boundary edges, is given by the Boltzmann ratio:

$$\frac{P(0 \rightarrow 4)}{P(0 \rightarrow 0)} = \frac{P(4 \rightarrow 4)}{P(4 \rightarrow 0)} = e^{-8\beta} \quad (\beta = 1/T), \quad (3.16)$$

where the energy cost along each edge is taken to be 2 (flipping  $-1$  to  $+1$  in the Gauss law term) and  $P(i \rightarrow j)$  stands for the unit-time transition probability (rate) from  $i$  violated edges to  $j$  violated edges. Note that both transition processes  $0 \rightarrow 4$  and  $4 \rightarrow 0$  can be induced by a “plaquette flipping” corresponding to a Pauli-Z operator  $Z_f$  acted on the qubit associated with the plaquette  $f$ . Similarly, the transition process between the configurations with 1 violated edge and 3 violated edges is also induced by a plaquette flipping, with the transition probability ratio given by:

$$\frac{P(1 \rightarrow 3)}{P(1 \rightarrow 1)} = \frac{P(3 \rightarrow 3)}{P(3 \rightarrow 1)} = e^{-4\beta}. \quad (3.17)$$

Finally, for all the configurations with two violated edges which have the same energy, one can set the plaquette flipping probability at unit time to be  $1/2$  which connects different configurations and ensures ergodicity (any initial configuration has a non-zero probability to reach any final configuration). As one can see, when the temperature  $T$  (and the thermal noise) is low enough, such local system-bath interaction will gradually shrink the perimeter of the loop excitations and suppress the error proliferation autonomously. This prevents a homologically non-trivial worldsheets of loop excitations being created which induces a logical error.

The critical temperature below which the loop excitation error is self-correcting is determined by the balance between the Boltzmann suppression  $e^{-2\beta\ell}$  for loop of length  $\ell$  and the loop entropy. The latter can be estimated from the self-avoiding random walk abundance  $n(\ell) \sim P(\ell)\mu^\ell$ , where  $P(\ell)$  is a polynomial and  $\mu$  is the connective constant on hypercubic lattice which is  $\mu \sim 8.84$  for 5-dimensional hypercubic lattice [37]. Thus the critical temperature below which the loop error is self correcting is given by

$$e^{-2\beta_c} \mu \geq 1 \Rightarrow T_c \geq \frac{2}{\log \mu k_B} \sim 0.92/k_B, \quad (3.18)$$

where  $\beta_c = 1/T_c$ ,  $k_B$  is the Boltzmann constant, and the energy is measured in the unit such that the smallest loop of four lattice edges has energy  $2 \times 4 = 8$ . The above analysis is for one type of loop excitation, but it applies to three types of loop excitations, where the probability combining the Boltzmann factor and the entropy is raised to the third power.

We note that the above analysis also equivalently establishes a probabilistic local cellular-automaton decoder for the loop excitation errors in the context of active error correction, where the local decoder simulates the local system-bath interaction. In particular, Eq. (3.16) and (3.17), along with the  $1/2$ -probability plaquette flipping for the configurations with two violated edges, define a local update rule of for the cellular-automaton decoder at each syndrome measurement cycle. Note that either the measurement or the recovery operation has certain error probability. An error threshold for this decoder can be obtained via the effective critical temperature:  $p_c \sim e^{-8\beta_c}$  [25]. Due to the local nature of the decoder, there is no non-local classical communication required in the decoding process, which hence does not lead to a classical communication/computation overhead as the system scales, in contrast to the case of the usual non-local decoders.

**Errors inducing membrane excitations** Now let us analyze the membrane excitation error in a similar manner. The smallest membrane excitation corresponds to violating the flux term on a cube  $s_3$ , which is a  $5 - 3 = 2$  dimensional membrane on the dual lattice. Let us consider the flux for  $a$ . Then the Gauss law term for  $b, c$  will have energy cost 1 for the edge  $s_1, s'_1$  such that  $\int \tilde{s}_3 \cup \tilde{s}_1 \cup \tilde{s}'_1 = 1$ . The cube  $s_3$  corresponds to one surface  $s_2$

such that  $\int \tilde{s}_3 \cup \tilde{s}_2 = 1$  on 5-dimensional hypercubic lattice, and the edges  $s_1, s'_1$  can be two ordered consecutive edges on the boundary of the surface  $s_2$ . Thus there are four Gauss law terms contribute to energy cost  $1 \times 4 = 4$ , with a total energy  $4 \times 1 + 2 \times 1 = 6$ , where the second term is from the flux term on the cube. The smallest membrane excitation created by a single Pauli  $X_f^i$ , say  $i = 1$ , consists of 6 cubes from the  $2 \times (5 - 2) = 6$  directions perpendicular to the face  $f$  in both positive and negative directions. Let us consider the following transition probabilities:

- Creation or survival of a small membrane excitation, i.e. fluxes on 6 cubes:

$$\frac{P(0 \rightarrow 6)}{P(0 \rightarrow 0)} = \frac{P(6 \rightarrow 6)}{P(6 \rightarrow 0)} = e^{-36\beta} . \quad (3.19)$$

- Deforming the membrane excitation with fluxes on  $1 \rightarrow 5$  cubes or  $5 \rightarrow 1$  cubes:

$$\frac{P(1 \rightarrow 5)}{P(1 \rightarrow 1)} = \frac{P(5 \rightarrow 5)}{P(5 \rightarrow 1)} = e^{-24\beta} . \quad (3.20)$$

- Deforming the membrane excitation with fluxes on  $2 \rightarrow 4$  cubes or  $4 \rightarrow 2$  cubes:

$$\frac{P(2 \rightarrow 4)}{P(2 \rightarrow 2)} = \frac{P(4 \rightarrow 4)}{P(4 \rightarrow 2)} = e^{-12\beta} . \quad (3.21)$$

- Deforming the membrane excitation with fluxes on  $3 \rightarrow 3$  cubes: one can set the cube flipping probability at unit time to be  $1/2$  which connects different configurations and ensures ergodicity.

To estimate the critical temperature, we will need to balance the Boltzmann suppression  $e^{-6\beta A}$  for membrane excitations of area  $A$  and the entropy of the membrane. The latter can be estimated from self-avoiding random surfaces on 5-dimensional hypercubic dual lattice, which is discussed in e.g. Ref. [64]. The abundance again grows as  $e^{A/\tau_0}$  for some constant  $\tau_0$ , thus the critical temperature is  $T'_c \geq 6\tau_0/k_B$ . A probabilistic cellular automaton decoder is also present for the membrane excitation errors, similar to the one discussed above for the loop excitation errors.

Combining the results from the loop and membrane excitations, for temperature below  $\min(T_c, T'_c)$ , the quantum memory is self-correcting.

Note that the above transition probabilities (Eq. (3.19) to (3.21) and the additional  $1/2$ -probability transition rule) also equivalently establish a probabilistic local cellular automaton decoder for the membrane excitation errors.

### 3.5.1 Readout of the memory and decoding the logical information

We have analyzed the error suppression during the process of the quantum computation, while there always exist residual errors that are never completely corrected. In the end of the quantum computation, we need to measure the encoded logical qubits in a certain logical basis. This can be done by performing a readout of all the qubits in a certain basis and then measure the corresponding logical operators. A convenient choice for this code is to measure all the qubits in the  $Z$  basis, which enables the measurement of electric Wilson membrane operators which have a product form  $\prod Z_f^i$ . Now in order to extract the encoded logical information, we assume that a reliable classical computer can help with decoding the measured classical data. Note that the measured data will contain errors originated from e.g. the thermal and readout noise. The errors in the Pauli- $Z$  measurement can be detected via the error syndromes corresponding to the Gauss term, i.e., loop excitations. We then apply the probabilistic local cellular automaton decoder (for the loop excitation errors) presented above to clean up the loop excitations. Since the classical computer is reliable, this recovery process can be executed perfectly. One can then perform a readout on the Wilson membrane operators  $\prod Z_f^i$ . Note that a logical error can occur if the above recovery process creates a homologically non-trivial worldsheet of the loop excitations. Such a logical error can be exponentially suppressed with the system size  $L$  when the bath temperature is below the critical temperature  $\min(T_c, T'_c)$  and the readout error is below the error threshold of this decoder  $p_c \sim e^{-8\beta c}$ .

### 3.5.2 Generalization: general cubic theory without particles

Let us generalize the argument to general cubic theory without particles, with  $m, n, D$  satisfying (2.18). The theory consists of electric excitations of  $(m-1), (n-1), (D-m-n-1) \geq 1$  dimensions and magnetic excitations of  $(D-m-2), (D-n-2), (m+n-2) \geq 1$  dimensions. The thermal stability depends on the balance between the Boltzmann suppression and the entropy.

- The energy cost for the  $k$ -dimensional electric excitations is  $2\epsilon_0 V_k$  where the Hamiltonian has coefficient  $\epsilon_0$  and  $V_k$  is the volume of the excitations in terms of the lattice spacing. The energy cost for the  $k'$ -dimensional magnetic excitations is  $(\epsilon_0 + 2\epsilon_0)V_{k'} = 3\epsilon_0 V_{k'}$ . The energy gap is thus bounded below by  $2\epsilon_0 V_k$  for  $k$ -dimensional excitation.
- The multiplicity of  $k$ -dimensional excitation of volume  $V_k$  for  $k \geq 1$  can be estimated as follows, following [25]. The first step of the random “submanifold-walk” on hypercubic lattice chooses  $k$  distinct directions out of  $2D$  directions (including the orientation),

and the next step one chooses a boundary of this  $k$ -simplex to attach with another  $k$ -simplex, thus one first makes a choice out of  $2k$  (including the orientation), and then one attaches to the original  $k$ -simplex with a new one by combining the boundary with one orthogonal direction not overlapping with the original  $k$ -simplex, which is a choice of  $2D - k$ . Thus the multiplicity of  $V_k$  steps is bounded above by

$$n(V_k) \leq 2D(2k(2D - k))^{V_k} . \quad (3.22)$$

To suppress large excitations, it is sufficient to require the temperature to be lower than  $1/(\beta k_B)$  where

$$e^{-\beta 2\epsilon_0 V_k} 2D(2k(2D - k))^{V_k} \sim 1 . \quad (3.23)$$

In other words, this gives an estimation of the critical temperature below which there are no large  $k$ -dimensional excitations

$$T_c(k) \sim \frac{2\epsilon_0}{\log(2k(2D - k))k_B} . \quad (3.24)$$

The critical temperature for all excitations is then

$$T_c \sim \min_{k \in \{(m-1), (n-1), (D-m-n-1), (D-m-2), (D-n-2), (m+n-2)\}} T_c(k) . \quad (3.25)$$

We remark that if  $k \rightarrow 0$ , i.e. particle excitations, the estimation gives  $T_c(k) \rightarrow 0$  and  $T_c \rightarrow 0$ , which is consistent with thermal instability for topological orders with particles.

## 4 Discussion and Outlook

In this work we have constructed a family of infinite many candidate non-Abelian self-correcting quantum memories in spacetime dimension  $D \geq 5 + 1$ , which is the dimension that the non-Abelian self-correcting memories can occur. These models also give rise to the first set of non-Abelian topological orders which are stable at finite temperature. The models can be described by three  $\mathbb{Z}_2$  higher-form gauge fields with cubic topological interaction among them. In these models, the electric excitations obey Abelian fusion rules, while the magnetic excitations obey non-Abelian fusion rules. We discuss the properties of the models using field theory and non-Pauli stabilizer lattice Hamiltonian models. We use a Peierls argument to show the self-correcting properties and thermal stability, and devise a probabilistic local cellular-automaton decoder for these codes.

There are several future directions. A more rigorous proof of the self-correcting properties based on Lindblad dynamics can be obtained in a similar way as Refs. [65, 30], since the error correction property of our commuting non-Pauli stabilizer model is very close to the 4D



CSS toric code. One can also develop a deterministic cellular-automaton decoder using non-equilibrium dynamics in analogy to Toom’s rule or sweep decoder [66], which is more efficient in cleaning up the errors than the current probabilistic decoder. Besides the study of the memory storage, the non-Abelian nature of this code can potentially allow us to perform non-Clifford and universal logical gate set in a self-correcting memory in five spatial dimensions, which would be lower dimensional than the current universal computation scheme with self-correcting memory based on a 6D color code [30]. Also, the distance scaling of the non-Abelian self-correcting memory  $d = O(N^{\frac{2}{5}})$  is better than that of the 6D color code  $d = O(N^{\frac{1}{3}})$  for total number of qubits equal  $N$ . Such fault-tolerant computing scheme will be highly desirable since it does not need non-local classical communication and there is no classical decoding overhead during the quantum computation process except the final readout stage when quantum operation already stops.

Finally, in our discussion we have focused on topological orders with fully-mobile excitations. It would be interesting to explore more general fractonic non-Abelian quantum memories in even lower spatial dimensions, where the code space can have exponentially many logical qubits in the system size.

## Acknowledgement

We thank Yu-An Chen and Nathanan Tantivasadakarn for discussions. We thank Maissam Barkeshli, Xie Chen, Meng Cheng, Shu-Heng Shao and Dominic J. Williamson for comments on a draft. P.-S.H. was supported by Simons Collaboration of Global Categorical Symmetry, Department of Mathematics King’s College London, and also supported in part by grant NSF PHY-2309135 to the Kavli Institute for Theoretical Physics (KITP). RK is supported by the JQI postdoctoral fellowship at the University of Maryland. GZ is supported by the U.S. Department of Energy, Office of Science, National Quantum Information Science Research Centers, Co-design Center for Quantum Advantage (C2QA) under contract number DE-SC0012704. P.-S.H. thanks Kavli Institute for Theoretical Physics for hosting the program “Correlated Gapless Quantum Matter” in 2024, during which part of the work is completed.

## A Obstruction to Non-Abelian Fusion

Let us generalize the argument in [31, 32] that rule out TQFTs with non-Abelian loop excitations in the absence of particles.

Consider TQFTs without  $(n - 1)$ -dimensional excitations, where we take  $n \geq 2$ . Suppose

there are  $n$ -dimensional simple excitations  $p_i$  with non-Abelian fusion rules on  $S^1 \times S^{n-1}$ :

$$p_1 \times p_2 = \sum_{i=3,4,\dots} p_i, \quad (\text{A.1})$$

where  $p_i$  can be the same when the multiplicity is greater than one. We can shrink the  $S^1$  to a point, then the  $n$ -dimensional excitations become  $(n-1)$ -dimensional excitations on  $S^{n-1}$ . For simple  $n$ -dimensional excitations, the reduction on a circle gives an excitation that contains at most one copy of identity. Since there is no nontrivial  $(n-1)$ -dimensional excitations, this gives only the identity. The fusion rule (A.1) becomes

$$1 \times 1 = \sum_{i=3,4,\dots} 1. \quad (\text{A.2})$$

Thus we have a contradiction unless there is only one term on the right hand side. In other words, the fusion of the  $n$ -dimensional excitations is Abelian.

## B Review of Cup Product on Triangulated and Hypercubic Lattices

Let us review cup product for  $\mathbb{Z}_2$  valued cochains on triangulated lattice and hypercubic lattice. For more details, see e.g. [67, 51–53, 22].

A  $\mathbb{Z}_2$ -valued  $m$ -cochain  $\alpha_m$  is a map from  $m$ -simplices on the lattice to  $0, 1 \pmod 2$ . The cup product of  $m$ -cochain  $\alpha_m$  and  $n$ -cochain  $\beta_n$  is an  $(m+n)$ -cochain  $\alpha_m \cup \beta_n$  defined as follows:

- For triangulated lattice, denote  $k$ -simplices by the vertices  $s_k = (0, 1, 2, 3, \dots, k)$ , the cup product takes the following value on  $(m+n)$ -simplices:

$$\alpha_m \cup \beta_n(0, 1, 2, \dots, m+n) = \alpha_m(0, 1, \dots, m) \beta_n(m, m+1, m+2, \dots, m+n). \quad (\text{B.1})$$

We note that there is a common vertex  $m$ .

- For hypercubic lattice, the cup product  $\alpha_m \cup \beta_n$  on  $(m+n)$ -dimensional hypercube  $s_{m+n}$  that span the coordinates  $(x^1, x^2, \dots, x^{m+n}) \in [0, 1]^{m+n}$  is given by

$$\alpha_m \cup \beta_n(s_{m+n}) = \sum_I \alpha_m([0, 1]^I) \beta_n\left((x^I = 1, x^{\bar{I}} = 0) + [0, 1]^{\bar{I}}\right), \quad (\text{B.2})$$

where the summation is over the different sets  $I$  of  $m$  coordinates out of the  $(m+n)$  coordinates  $x^1, \dots, x^{m+n}$ ,  $\bar{I}$  denotes the remaining  $n$  coordinates. In each term in the sum,  $\alpha_m, \beta_n$  are evaluated on an  $m$ -dimensional hypercube and an  $n$ -dimensional hypercube, where the two hypercubes intersect at a point  $(x^I = 1, x^{\bar{I}} = 0)$ :

- $[0, 1]^I$  is the  $m$ -dimensional unit hypercube starting from  $(x^I = 0, x^{\bar{I}} = 0)$  and ending at  $(x^I = 1, x^{\bar{I}} = 0)$ , i.e.  $[0, 1]^I = \{0 \leq x^i \leq 1, x^j = 0 : i \in I, j \in \bar{I}\}$ .
- $(x^I = 1, x^{\bar{I}} = 0) + [0, 1]^{\bar{I}}$  is the  $n$ -dimensional hypercube in the  $\bar{I}$  directions starting from  $(x^I = 1, x^{\bar{I}} = 0)$  and ending at  $(x^I = 1, x^{\bar{I}} = 1)$ , i.e.  $(x^I = 1, x^{\bar{I}} = 0) + [0, 1]^{\bar{I}} = \{x^i = 1, 0 \leq x^j \leq 1 : i \in I, j \in \bar{I}\}$ .

## C Logical CZ, S, Hadamard Gates in 4D Loop Toric Code

We will discuss the logical gates in the loop toric code model in 4+1d, which is an example of self-correcting quantum memory at finite temperature (e.g. [25, 5]). The Hamiltonian is a stabilizer model:

$$H = H_{\text{Gauss}} + H_{\text{Flux}} = - \sum_e \prod_{f \in \partial e} X_f - \sum_c \prod_{f \in \partial c} Z_f, \quad (\text{C.1})$$

where the  $\mathbb{Z}_2$  2-form gauge field is  $a_f = (1 - Z_f)/2$ . The ground states on  $M_4$  4-manifold is given by  $q$  qubits with  $H^2(M_4, \mathbb{Z}_2) = \mathbb{Z}_2^q$ .

The loop toric code has loop excitations labelled by the electric and magnetic charges  $(q_e, q_m)$  with  $q_e, q_m = 0, 1$ , i.e. pure electric loop  $(1, 0)$ , pure magnetic loop  $(0, 1)$  and dyon loop  $(1, 1)$ , corresponding to violation of the Gauss law terms along the loop, flux terms along the loop and both types of Hamiltonian terms along the loop.

### C.1 Hadamard gate

The model on hypercubic lattice has electromagnetic duality spin rotation symmetry that exchanges  $X \leftrightarrow Z$ , and swaps the lattice with the dual lattice. To see this, we note that the Gauss law term on edge in the  $x$  direction has product over  $X_f$  spanning  $x$  direction and one of the remaining  $4 - 1 = 3$  directions, and taking into account the orientation the product is over  $3 \times 2 = 6 X_f$ . Similarly, each cube  $c$  spanning  $x, y, z$  directions has faces in  $xy, yz, zx$  directions, with orientations there are in total  $3 \times 2 = 6 Z_f$  in the product of each flux term.

On the loop excitations the symmetry acts as  $S : (q_e, q_m) \leftrightarrow (q_m, q_e)$ , where we note  $-q_m = q_m \pmod{2}$ , as well as  $T : (q_e, q_m) \rightarrow (q_e + q_m, q_m)$  [68, 22]. The  $S$  symmetry acts as Hadamard gate.

## C.2 CZ and S gates

The  $T : (q_e, q_m) \rightarrow (q_e + q_m, q_m)$  symmetry is generated by the gauged SPT defect decorated with  $H^4(B^2\mathbb{Z}_2, U(1)) = \mathbb{Z}_4$ : [22]

$$U(M_4) = i^{\int \mathcal{P}(a)} . \quad (\text{C.2})$$

The gauged SPT phase on the domain wall is the semion Walker Wang model. The operator acting the ground states labelled by holonomy  $\{n_i = 0, 1\}$  for  $i = 1, 2, \dots, q$  according to the intersection form  $M_{ij}$  on  $H^2(M_4)$ :

$$U(M_4)|\{n_i\}\rangle = i^{\sum_j M_{jj}n_j^2} (-1)^{\sum_{i < j} M_{ij}n_i n_j} |\{n_i\}\rangle . \quad (\text{C.3})$$

Consider the following cases:

- $M_4 = T_{x,y,z,w}^4$ , with  $q = 6$ . The operator realizes the logical gate

$$U(T^4) = \text{CZ}_{xy,zw} \text{CZ}_{xz,yw} \text{CZ}_{yz,xw} , \quad (\text{C.4})$$

where  $xy$  is the 2-cycle spanning  $x, y$  directions, and similarly for  $zw, xz, yw, yz, xw$ .

In particular, this implies that  $U(T^4)X_{xy}U(T^4)^{-1} = X_{xy}Z_{zw}$ , where  $X, Z$  are the logical gates. Thus the symmetry permutes the magnetic loop excitation to the dyon loop excitation. This is the case considered in [22].

- $M_4 = \mathbb{CP}^2$ , with  $q = 1$ . The operator realizes the logical gate

$$U(T^4) = S . \quad (\text{C.5})$$

In other words, if the state has trivial holonomy on the 2-cycle, the operator acts trivially; if the state has nontrivial holonomy on the 2-cycle, the operator acts as  $i$ .

## References

- [1] M. Iqbal *et al.*, “Non-Abelian topological order and anyons on a trapped-ion processor,” *Nature* **626** no. 7999, (2024) 505–511, arXiv:2305.03766 [quant-ph].
- [2] Z. Nussinov and G. Ortiz, “Autocorrelations and thermal fragility of anyonic loops in topologically quantum ordered systems,” *Physical Review B* **77** no. 6, (Feb., 2008) . <http://dx.doi.org/10.1103/PhysRevB.77.064302>.
- [3] S. Bravyi and B. Terhal, “A no-go theorem for a two-dimensional self-correcting quantum memory based on stabilizer codes,” *New Journal of Physics* **11** no. 4, (Apr., 2009) 043029. <http://dx.doi.org/10.1088/1367-2630/11/4/043029>.

- [4] M. B. Hastings, “Topological order at nonzero temperature,” *Phys. Rev. Lett.* **107** (Nov, 2011) 210501.  
<https://link.aps.org/doi/10.1103/PhysRevLett.107.210501>.
- [5] B. J. Brown, D. Loss, J. K. Pachos, C. N. Self, and J. R. Wootton, “Quantum memories at finite temperature,” *Reviews of Modern Physics* **88** no. 4, (Nov., 2016) .  
<http://dx.doi.org/10.1103/RevModPhys.88.045005>.
- [6] L. Guth and A. Lubotzky, “Quantum error correcting codes and 4-dimensional arithmetic hyperbolic manifolds,” *Journal of Mathematical Physics* **55** no. 8, (2014) 082202.
- [7] N. P. Breuckmann and V. Londe, “Single-Shot Decoding of Linear Rate LDPC Quantum Codes with High Performance,” *arXiv quant-ph* (2020) , 2001.03568.
- [8] M. Freedman and M. B. Hastings, “Building manifolds from quantum codes,” *arXiv:2012.02249* (2020) .
- [9] S. Bravyi, A. W. Cross, J. M. Gambetta, D. Maslov, P. Rall, and T. J. Yoder, “High-threshold and low-overhead fault-tolerant quantum memory,” *Nature* **627** no. 8005, (2024) 778–782. <https://doi.org/10.1038/s41586-024-07107-7>.
- [10] N. P. Breuckmann, C. Vuillot, E. Campbell, A. Krishna, and B. M. Terhal, “Hyperbolic and semi-hyperbolic surface codes for quantum storage,” *Quantum Science and Technology* **2** no. 3, (Aug., 2017) 035007–21.
- [11] M. Hastings, J. Haah, and R. O’Donnell, “Fiber bundle codes: breaking the  $n^{1/2}$ polylog( $n$ ) barrier for quantum ldpc codes,” in *Proc. ACM STOC*, pp. 1276–1288. Association for Computing Machinery, New York, NY, USA, 2021.
- [12] P. Panteleev and G. Kalachev, “Quantum ldpc codes with almost linear minimum distance,” *IEEE Trans. Inf. Theo.* **68** no. 1, (2022) 213–229.
- [13] N. P. Breuckmann and J. N. Eberhardt, “Balanced product quantum codes,” *IEEE Trans. Inf. Theo.* **67** no. 10, (2021) 6653–6674.
- [14] M. Hastings, “On quantum weight reduction,” *arXiv:2102.10030* (2021) .
- [15] P. Panteleev and G. Kalachev, “Asymptotically good quantum and locally testable classical ldpc codes,” in *Proc. ACM STOC*, pp. 375—388. Association for Computing Machinery, New York, NY, USA, 2022.
- [16] A. Leverrier and G. Zemor, “Quantum tanner codes,” in *Proc. IEEE FOCS*, pp. 872–883. IEEE Computer Society, Los Alamitos, CA, USA, 2022.  
<https://doi.ieeecomputersociety.org/10.1109/FOCS54457.2022.00117>.
- [17] T. Lin and M. Hsieh, “Good quantum ldpc codes with linear time decoder from lossless expanders,” *arXiv:2203.03581* (2022) .

- [18] S. Gu, C. Pattison, and E. Tang, “An efficient decoder for a linear distance quantum ldpc code,” *arXiv:2206.06557* (2022) .
- [19] I. Dinur, M. Hsieh, T. Lin, and T. Vidick, “Good quantum ldpc codes with linear time decoders,” in *Proc. ACM STOC*, pp. 905–918. Association for Computing Machinery, New York, NY, USA, 2023.
- [20] A. Leverrier and G. Zémor, *Efficient decoding up to a constant fraction of the code length for asymptotically good quantum codes*, pp. 1216–1244. 2023.  
<https://epubs.siam.org/doi/abs/10.1137/1.9781611977554.ch45>.
- [21] S. Gu, E. Tang, L. Caha, S. Choe, Z. He, and A. Kubica, “Single-shot decoding of good quantum ldpc codes,” *arXiv:2306.12470* (2023) .
- [22] X. Chen, A. Dua, P.-S. Hsin, C.-M. Jian, W. Shirley, and C. Xu, “Loops in 4+1d Topological Phases,” *arXiv:2112.02137* [cond-mat.str-el].
- [23] B. Yoshida, “Feasibility of self-correcting quantum memory and thermal stability of topological order,” *Annals of Physics* **326** no. 10, (Oct., 2011) 2566–2633.  
<http://dx.doi.org/10.1016/j.aop.2011.06.001>.
- [24] E. T. Campbell, B. M. Terhal, and C. Vuillot, “Roads towards fault-tolerant universal quantum computation,” *Nature* **549** no. 7671, (09, 2017) 172–179.
- [25] E. Dennis, A. Kitaev, A. Landahl, and J. Preskill, “Topological quantum memory,” *J. Math. Phys.* **43** (2002) 4452–4505, *arXiv:quant-ph/0110143*.
- [26] H. Bombin, “Single-shot fault-tolerant quantum error correction,” *Phys. Rev. X* **5** no. 3, (2015) 031043.
- [27] G. Zhu, A. Lavasani, and M. Barkeshli, “Universal logical gates on topologically encoded qubits via constant-depth unitary circuits,” *Phys. Rev. Lett.* **125** (Jul, 2020) 050502. <https://link.aps.org/doi/10.1103/PhysRevLett.125.050502>.
- [28] G. Zhu, A. Lavasani, and M. Barkeshli, “Instantaneous braids and dehn twists in topologically ordered states,” *Phys. Rev. B* **102** (Aug, 2020) 075105.  
<https://link.aps.org/doi/10.1103/PhysRevB.102.075105>.
- [29] A. Lavasani, G. Zhu, and M. Barkeshli, “Universal logical gates with constant overhead: instantaneous dehn twists for hyperbolic quantum codes,” *Quantum* **3**, 180 (2019) .
- [30] H. Bombin, R. W. Chhajlany, M. Horodecki, and M. A. Martin-Delgado, “Self-correcting quantum computers,” *New Journal of Physics* **15** no. 5, (May, 2013) 055023–44.
- [31] T. Johnson-Freyd and M. Yu, “Topological Orders in (4+1)-Dimensions,” *SciPost Phys.* **13** no. 3, (2022) 068, *arXiv:2104.04534* [hep-th].

- [32] C. Cordova, P.-S. Hsin, and C. Zhang, “Anomalies of Non-Invertible Symmetries in  $(3+1)d$ ,” [arXiv:2308.11706 \[hep-th\]](#).
- [33] L. Kong and X.-G. Wen, “Braided fusion categories, gravitational anomalies, and the mathematical framework for topological orders in any dimensions,” [arXiv:1405.5858 \[cond-mat.str-el\]](#).
- [34] L. Kong, X.-G. Wen, and H. Zheng, “Boundary-bulk relation for topological orders as the functor mapping higher categories to their centers,” 2015.
- [35] L. Kong, X.-G. Wen, and H. Zheng, “Boundary-bulk relation in topological orders,” *Nuclear Physics B* **922** (Sept., 2017) 62–76.  
<http://dx.doi.org/10.1016/j.nuclphysb.2017.06.023>.
- [36] T. Johnson-Freyd, “On the classification of topological orders,” *Communications in Mathematical Physics* **393** no. 2, (Apr., 2022) 989–1033.  
<http://dx.doi.org/10.1007/s00220-022-04380-3>.
- [37] N. Madras and G. Slade, *The Self-Avoiding Walk*. Modern Birkhäuser Classics. Springer New York, 2012. <https://books.google.com/books?id=xo32YMg1D0cC>.
- [38] M. de Wild Propitius, “Confinement in partially broken abelian chern-simons theories,” *Physics Letters B* **410** no. 2, (1997) 188–194.  
<https://www.sciencedirect.com/science/article/pii/S0370269397009854>.
- [39] A. Coste, T. Gannon, and P. Ruelle, “Finite group modular data,” *Nucl. Phys. B* **581** (2000) 679–717, [arXiv:hep-th/0001158](#).
- [40] P.-S. Hsin and A. Turzillo, “Symmetry-enriched quantum spin liquids in  $(3 + 1)d$ ,” *JHEP* **09** (2020) 022, [arXiv:1904.11550 \[cond-mat.str-el\]](#).
- [41] M. Barkeshli, Y.-A. Chen, P.-S. Hsin, and R. Kobayashi, “Higher-group symmetry in finite gauge theory and stabilizer codes,” *SciPost Phys.* **16** (2024) 089, [arXiv:2211.11764 \[cond-mat.str-el\]](#).
- [42] E. Witten, “Five-brane effective action in M theory,” *J. Geom. Phys.* **22** (1997) 103–133, [arXiv:hep-th/9610234](#).
- [43] E. Witten, “AdS / CFT correspondence and topological field theory,” *JHEP* **12** (1998) 012, [arXiv:hep-th/9812012](#).
- [44] E. Witten, “Geometric Langlands From Six Dimensions,” [arXiv:0905.2720 \[hep-th\]](#).
- [45] D. S. Freed and C. Teleman, “Relative quantum field theory,” *Commun. Math. Phys.* **326** (2014) 459–476, [arXiv:1212.1692 \[hep-th\]](#).
- [46] C. Córdova, D. Costa, and P.-S. Hsin. To appear.

- [47] B. Yoshida, “Topological color code and symmetry-protected topological phases,” *Phys. Rev. B* **91** (Jun, 2015) 245131.  
<https://link.aps.org/doi/10.1103/PhysRevB.91.245131>.
- [48] B. Yoshida, “Topological phases with generalized global symmetries,” *Phys. Rev. B* **93** (Apr, 2016) 155131. <https://link.aps.org/doi/10.1103/PhysRevB.93.155131>.
- [49] B. Yoshida, “Gapped boundaries, group cohomology and fault-tolerant logical gates,” *Annals of Physics* **377** (2017) 387–413.  
<https://www.sciencedirect.com/science/article/pii/S0003491616302858>.
- [50] M. Barkeshli, Y.-A. Chen, S.-J. Huang, R. Kobayashi, N. Tantivasadakarn, and G. Zhu, “Codimension-2 defects and higher symmetries in (3+ 1) d topological phases,” *SciPost Physics* **14** no. 4, (2023) 065.
- [51] F. Benini, C. Córdova, and P.-S. Hsin, “On 2-Group Global Symmetries and their Anomalies,” *JHEP* **03** (2019) 118, [arXiv:1803.09336](https://arxiv.org/abs/1803.09336) [hep-th].
- [52] L. Tsui and X.-G. Wen, “Lattice models that realize  $F_{n-1}$  symmetry-protected topological states for even  $n$ ,” *Phys. Rev. B* **101** (Jan, 2020) 035101.
- [53] Y.-A. Chen and S. Tata, “Higher cup products on hypercubic lattices: application to lattice models of topological phases,” [arXiv:2106.05274](https://arxiv.org/abs/2106.05274) [cond-mat.str-el].
- [54] X. Chen, Z.-C. Gu, Z.-X. Liu, and X.-G. Wen, “Symmetry protected topological orders and the group cohomology of their symmetry group,” *Phys. Rev. B* **87** no. 15, (2013) 155114, [arXiv:1106.4772](https://arxiv.org/abs/1106.4772) [cond-mat.str-el].
- [55] L. Tsui and X.-G. Wen, “Lattice models that realize  $\mathbb{Z}_n$ -1 symmetry-protected topological states for even  $n$ ,” *Phys. Rev. B* **101** no. 3, (2020) 035101, [arXiv:1908.02613](https://arxiv.org/abs/1908.02613) [cond-mat.str-el].
- [56] M. Levin and Z.-C. Gu, “Braiding statistics approach to symmetry-protected topological phases,” *Phys. Rev. B* **86** (Sep, 2012) 115109.  
<https://link.aps.org/doi/10.1103/PhysRevB.86.115109>.
- [57] L. Bhardwaj, D. Gaiotto, and A. Kapustin, “State sum constructions of spin-TFTs and string net constructions of fermionic phases of matter,” *JHEP* **04** (2017) 096, [arXiv:1605.01640](https://arxiv.org/abs/1605.01640) [cond-mat.str-el].
- [58] W. Shirley, K. Slagle, and X. Chen, “Foliated fracton order from gauging subsystem symmetries,” *SciPost Phys.* **6** no. 4, (2019) 041, [arXiv:1806.08679](https://arxiv.org/abs/1806.08679) [cond-mat.str-el].
- [59] A. Kubica, B. Yoshida, and F. Pastawski, “Unfolding the color code,” *New J. Phys.* **17** no. 8, (2015) 083026, [arXiv:1503.02065](https://arxiv.org/abs/1503.02065) [quant-ph].



- [60] H. Bombin and M. A. Martin-Delgado, “Topological quantum distillation,” *Phys. Rev. Lett.* **97** (2006) 180501, [arXiv:quant-ph/0605138](#).
- [61] G. Zhu, S. Sikander, E. Portnoy, A. W. Cross, and B. J. Brown, “Non-clifford and parallelizable fault-tolerant logical gates on constant and almost-constant rate homological quantum ldpc codes via higher symmetries,” *arXiv preprint arXiv:2310.16982* (2023) .
- [62] M. Barkeshli, P.-S. Hsin, and R. Kobayashi, “Higher-group symmetry of (3+1)D fermionic  $\mathbb{Z}_2$  gauge theory: logical CCZ, CS, and T gates from higher symmetry,” *SciPost Phys.* **16** (2024) 122, [arXiv:2311.05674 \[cond-mat.str-el\]](#).
- [63] P. Putrov, J. Wang, and S.-T. Yau, “Braiding Statistics and Link Invariants of Bosonic/Fermionic Topological Quantum Matter in 2+1 and 3+1 dimensions,” *Annals Phys.* **384** (2017) 254–287, [arXiv:1612.09298 \[cond-mat.str-el\]](#).
- [64] B. Durhuus, J. Fröhlich, and T. Jonsson, “Self-avoiding and planar random surfaces on the lattice,” *Nuclear Physics B* **225** no. 2, (1983) 185–203.  
<https://www.sciencedirect.com/science/article/pii/0550321383900482>.
- [65] R. Alicki, M. Horodecki, P. Horodecki, and R. Horodecki, “On thermal stability of topological qubit in kitaev’s 4d model,” *Open Systems & Information Dynamics* **17** no. 01, (2010) 1–20.
- [66] A. Dua, T. Jochym-O’Connor, and G. Zhu, “Quantum error correction with fractal topological codes,” *Quantum* **7** (2023) 1122.
- [67] J. Milnor, J. Stasheff, J. Stasheff, and P. University, *Characteristic Classes*. Annals of mathematics studies. Princeton University Press, 1974.  
<https://books.google.com/books?id=5zQ9AFk1i4EC>.
- [68] D. Gaiotto, A. Kapustin, N. Seiberg, and B. Willett, “Generalized Global Symmetries,” *JHEP* **02** (2015) 172, [arXiv:1412.5148 \[hep-th\]](#).